Heterogeneous Catalysis

DOI: 10.1002/ange.201403094

Revealing the Dynamic Structure of Complex Solid Catalysts Using Modulated Excitation X-ray Diffraction**

Davide Ferri, Mark A. Newton,* Marco Di Michiel,* Gian Luca Chiarello, Songhak Yoon, Ye Lu, and Jérôme Andrieux*

Abstract: *X-ray diffraction (XRD) is typically silent towards information on low loadings of precious metals on solid catalysts because of their finely dispersed nature. When combined with a concentration modulation approach, time-resolved high-energy XRD is able to provide the detailed redox dynamics of palladium nanoparticles with a diameter of 2 nm in 2 wt% Pd/CZ (CZ = ceria–zirconia), which is a difficult sample for extended X-ray absorption fine structure (EXAFS) measurements because of the cerium component. The temporal evolution of the Pd(111) and Ce(111) reflections together with surface information from synchronous diffuse reflectance infrared Fourier transform spectroscopy (DRIFTS) measurements reveals that Ce maintains Pd oxidized in the CO pulse, whereas reduction is detected at the beginning of the O_2 pulse. Oxygen is likely transferred from Pd to Ce^{3+} before the onset of Pd re-oxidation. In this context, adsorbed carbonates appear to be the rate-limiting species for re-oxidation.*

Establishing the structure of functional materials and the structural changes that occur whilst they are operating with the highest level of precision is a considerable research challenge. This key issue spans a vast range of disciplines as it is fundamental to both practical applications and our understanding of why materials behave as they do. X-ray diffraction (XRD)[1] and X-ray absorption spectroscopy (XAS)[2] as well as advanced microscopy[3] continue to be at the forefront of this endeavor. This task is made more challenging by the necessity to be able to observe structural changes while materials are functioning (in situ or operando conditions). Recently, progress has been made in utilizing approaches that are based on lock-in amplification to greatly enhance the sensitivity of such advanced probes[4–7] and to resolve aspects of the material behavior that would otherwise remain extremely difficult or even impossible to observe using conventional analytical approaches.

Synchrotron high-energy X-ray diffraction (HXRD) can provide adequate time resolution to follow kinetic processes on sub-second timescales.[8] This approach can permit insights into the behavior of a support material, the promoter phases, and the catalytically active precious-metal phase in a single shot. However, for many catalyst formulations, XRD is of reduced utility because of the low levels of structural order, domain sizes that are often limited to lengths below approximately 5 nm, and complex multiphasic patterns, which are extremely difficult to disentangle to yield the desired structural precision.[9] Practically, only the response of the catalyst support can often be recorded, unless larger precious-metal particles/oxide phases are present. This detection limit issue may be circumvented by increasing the metal loading to capture the dynamics of the precious-metal active phase;[10] however, this is only possible at the expense of the possibility to study technical catalysts working under representative conditions.

Herein, we demonstrate how a modulation approach coupled to phase-sensitive detection (PSD)[4a,11] can be applied to a working catalyst using time-resolved HXRD in combination with XAS, infrared spectroscopy, and mass spectrometry to observe and start to quantify aspects of the synergetic behavior between nanoscale Pd^0/Pd^{2+} entities at a low loading (2 wt%) on a ceria–zirconia (CZ) support material. Ceria-based catalysts are widely used in catalysis.[12] Ceria is a crucial component of three-way catalysts for automotive pollution control operating under fast periodic redox fluctuations.[12a] The Ce^{4+}/Ce^{3+} redox pair directs the buffering of oxygen during the short fuel-rich periods of operation. This function is absolutely central to maintaining an efficient catalytic operation and is typically probed by alternating CO and O_2 pulses. The interface that is achieved through contact of the metal nanoparticles with ceria, together with the availability of oxygen under fuel-rich conditions, curtails catalyst deactivation and specifically promotes or retards more fundamental aspects of the chemistry occurring on the metallic component.[13] The nature of the Pd/CZ system, namely the small amount and

[*] Dr. D. Ferri
Paul Scherrer Institut, 5232 Villigen PSI (Switzerland)
E-mail: davide.ferri@psi.ch
Dr. G. L. Chiarello,[+] Dr. S. Yoon, Dr. Y. Lu
Empa, Swiss Federal Laboratories for Materials Science and Technology, Laboratory for Solid State Chemistry and Catalysis
Ueberlandstrasse 129, 8600 Dübendorf (Switzerland)
Dr. M. A. Newton, Dr. M. Di Michiel, Dr. J. Andrieux[++]
ESRF, 71 Rue des Martyrs, 38000 Grenoble (France)
E-mail: mark.newton@esrf.fr
dimichie@esrf.fr
[+] Present address: Dipartimento di Chimica
Università degli Studi di Milano
Via C. Golgi 19, 20133 Milano (Italy)
[++] Present address: Université de Lyon
43 Bd du 11 Nov. 1918, 69622 Villeurbanne (France)

[**] This work was supported by the Competence Centre for Materials Science and Technology (CCMX) and the Swiss National Science Foundation (SNF; project 200021-138068). We thank ESRF for beam time allocation at beamlines ID15B and BM23, Umicore for kindly providing catalyst samples, and Dr. S. K. Matam and Dr. D. Zurita for help during beamtime.

Supporting information for this article is available on the WWW under http://dx.doi.org/10.1002/anie.201403094.

size of the Pd component, together with the highly absorbing/scattering nature of ceria itself has made it extremely difficult to obtain a detailed understanding of the structure–function relationships and the kinetics of the processes that define its superior behavior. We show that by using HXRD in tandem with the modulation approach and PSD, we can go considerably beyond what has been previously attained in related systems.[13b] We were able to follow some extremely subtle structure–reactivity changes that are at the very heart of the superior properties of these complex materials.

The color map representation of a CO/O_2 concentration modulation experiment carried out with 2.2 wt% Pd/CZ at 573 K is shown Figure 1 a. The concentrations of CO and O_2 in He are periodically and alternately switched between 0 and 1 vol% every 25 seconds. The sample (67 $m^2 g^{-1}$; 85% Pd dispersion)[14] is characterized by a highly dispersed Pd–O phase as demonstrated by the analysis of the local Pd environment using XAS (Supporting Information, Figure S1); this phase is also extremely challenging to observe by electron microscopy (Figure S2).[14] The time-resolved HXRD data of Figure 1 b present virtually no visible change, except for an extremely faint variation in the reflections of cubic CZ. No reflection of a palladium-containing phase was detectable using common XRD software.

The subtle changes induced by the CO/O_2 pulses were greatly enhanced by PSD. A set of phase-resolved data shows a subset of reflections of very low intensity that can now be readily discerned and associated with the temporal response of CZ (Figure 1 c). Their differential profile reflects a reversible shift of the CZ d spacing in response to the environment. This is indicative of a reversible lattice contraction/expansion as a consequence of oxygen removal and re-insertion, respectively.[13b] The amplitude of the change that is now visible is approximately 60 times lower than the intensity of the Bragg reflections that were observed in the time-resolved data.

More importantly, a second subset of reflections also appeared, which were completely invisible in the raw HXRD data. The signal at 2.78 $Å^{-1}$, which experiences only an intensity variation, is not characteristic of CZ. Further inspection of the PSD data revealed that the signal is accompanied by a series of further features at approximately 3.2, 4.5, 5.3, and 5.6 $Å^{-1}$, which overlap with the CZ reflections. A comparison with the JCPDS reference cards confirms that this set of signals corresponds to metallic Pd ((111), (200), (220), (311), and (222), respectively). This is further corroborated by a comparison with the PSD data obtained for a relatively simple system, insofar as Pd/Al_2O_3 can be considered as such. For 2 wt% Pd/Al_2O_3 (135 $m^2 g^{-1}$; 20% Pd dispersion, 5.6 nm mean particle size),[6a] both PdO and metallic Pd phases were clearly detected and already evident in the conventional time-resolved data (Figure 1 d–f). Conventional XRD is clearly sufficient to access detailed structure–reactivity kinetics of the dominant (Pd/PdO) redox couple (Figure 1 e). In this case, PSD revealed only intensity variations of the PdO and Pd reflections. Therefore, in a system that is very difficult to study with time-resolved spectroscopy, such as Pd/CZ, the formation of a metallic Pd phase during the CO pulse becomes visible only after application of PSD.

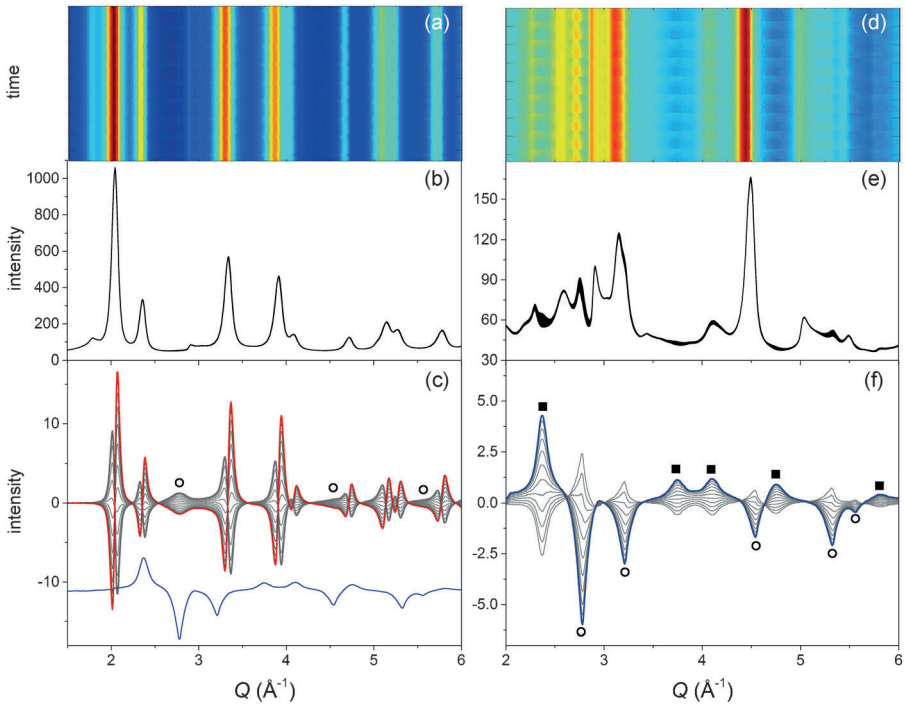

Figure 1. a) Color map representation and b) time-resolved hard XRD patterns for 2 wt% Pd/CZ during a full CO/O_2 modulation experiment at 573 K ($t = 50$ s). c) Corresponding set of phase-resolved data ($\phi^{PSD} = 10$–$150°$); the red profile is the in-phase pattern. The blue profile is the in-phase pattern obtained for 2 wt% Pd/Al_2O_3. d–f) High-energy XRD data for an identical experiment performed with 2 wt% Pd/Al_2O_3 ($\phi^{PSD} = 70$–$180°$). ○: Pd; ■: PdO.

The assignment of the reflections at 2.78 $Å^{-1}$ and at higher Q values to metallic Pd is further validated by the observation that palladium-free CZ does not exhibit any changes in the Q range corresponding to the Pd phase at 573 K (Figure S3). Furthermore, the amplitude of the changes observed for CZ on Pd/CZ is two orders of magnitude larger than in the absence of Pd, thus demonstrating a pronounced enhancement of ceria reduction by Pd, which is induced by the intimate contact of the two phases.[13b] However, PSD of the time-resolved data of Pd/CZ fails to provide any evidence for the participation of a PdO phase. Aside from the overlap with the CZ reflections, the most probable reason for the absence of the PdO reflections from PSD is that a defined phase

having the structural character of PdO does not form at all in the presence of CZ, which is consistent with the XAS analysis (Figure S1).

Based on the only clearly accessible reflection that corresponds to the formation of the metallic Pd phase [Pd(111), 2.78 $Å^{-1}$], the crystallite size was estimated by the Scherrer equation for the PSD data exhibiting the largest amplitude at 2.78 $Å^{-1}$ ($\phi^{PSD} = 180°$). A value of 1.9 nm was obtained, which is below the conventional threshold of XRD for this metal loading.[15] For the use of the Scherrer formula, it is assumed that strain does not contribute to the observed changes. Conventional strain analysis of the Pd/CZ material is hindered because only the Pd(111) reflection is clearly available. The mean particle size of 5.3 nm obtained with the same procedure for a number of reflections of Pd/Al_2O_3 corresponding to the PdO and Pd phases is in line with the chemisorption data (see above) and validates the XRD analysis. The simulated diffraction patterns of Pd nanoparticles with a diameter of 1–5 nm (Figure 2) confirmed that the signal observed in the phase-resolved data of Pd/CZ corresponds to a nanoparticle size of approximately to 2 nm, which is in striking agreement with the value obtained from the Scherrer equation. Similarly, the width at half height of the in-phase data of Pd/Al_2O_3 is also very close to that of the 5 nm particles.

The shift of the CZ pattern to low and high Q values upon CO and O_2 pulsing, which was clearly observed in the PSD data, is associated with the partial reduction of Ce^{4+} by CO. The data shown in Figure 1 indicate that the process that is observed under these experimental conditions is not a bulk reduction. Following the approach of Martorana et al.,[16] we have determined the fraction of Ce^{4+} that has been reduced by CO. The reliability of this method was confirmed by the measure of the mole content of Ce^{4+} (0.54), which was obtained by assuming only a cubic structure for CZ, which is compatible with the original CZ composition ($Ce_{0.6}Zr_{0.4}O_2$). The small discrepancy in the amount of cerium may lie in a small contribution of the tetragonal phase.[16] The very small shift in the d spacing (0.11% measured at 573 K (Figure S4)) indicates that only about 6% of the Ce^{4+} ions are reduced to Ce^{3+} (Figure 3a).[16] Therefore, the observed structural changes are caused by extremely subtle variations in the oxygen stoichiometry.

The dynamic changes that are associated with the Pd and CZ reflections and identified by PSD can be followed in a temporal manner, thus placing us in a position to extract reduction and re-oxidation kinetics. Figure 3b shows that in case of Pd/CZ, always the same fraction of Pd atoms responds to the periodic external stimulus, the extent of change remaining constant over the modulation periods. In strong contrast, the Pd(111) reflection of Pd/Al_2O_3 oscillates around a constant term only after the

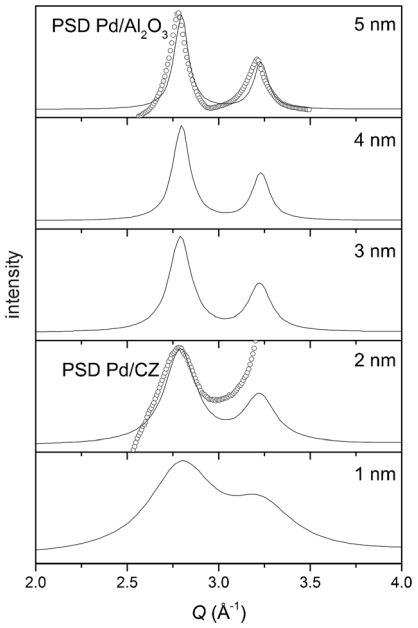

Figure 2. Pd(111) and Pd(200) regions of simulated XRD patterns for Pd nanoparticles with diameters of 1–5 nm. The symbols correspond to the in-phase data of Figure 1c (Pd/CZ) and Figure 1f (Pd/Al_2O_3), respectively, and are cut for simplicity. The contribution of CZ to the PSD data of Pd/CZ prevents the detection of the Pd(200) reflection.

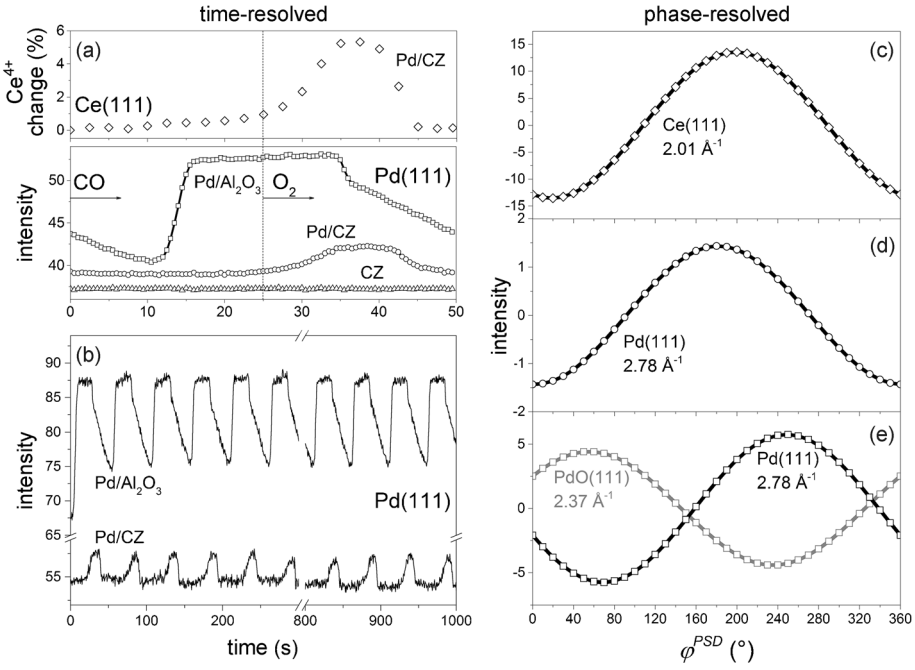

Figure 3. Left panel: temporal responses of the XRD reflections at $Q = 2.78$ $Å^{-1}$ (Pd(111)) over a) one modulation period (averaged data) and b) the whole CO/O_2 modulation experiment for Pd/CZ, Pd/Al_2O_3, and CZ. The fraction of reduced Ce^{4+} (Pd/CZ) over the modulation period is also shown in (a). Right panel: phase-angle (ϕ^{PSD}) dependence of selected reflections of c, d) Pd/CZ and e) Pd/Al_2O_3.

first CO pulse, revealing that re-oxidation is not able to completely restore the initial structure of the catalyst, which might be due to particle-size effects and the kinetics of the re-oxidation. Figure 3a also shows the temporal response of the signal at 2.78 $Å^{-1}$ for Pd/CZ and CZ and for Pd/Al_2O_3 for comparison, averaged over all modulation periods. The temporal profile of the CZ reflections is exemplarily represented by that at 2.01 $Å^{-1}$ and demonstrates that the d spacing variation, which corresponds to the $Ce^{4+} \rightarrow Ce^{3+}$ reduction, is synchronous to reduction of Pd^{2+}. However, detection of the Pd metal phase by XRD is delayed with respect to CO admittance,[16] and significantly retarded compared to the earlier reduction of Pd/Al_2O_3.

The absence of any response in the CO pulse, despite the detection of adsorbed CO in the synchronous DRIFT spectra (Figure S5), indicates that CO consumes the available oxygen provided by ceria within the reduction pulse. This matches the broad gaseous CO_2 profile observed by DRIFT spectroscopy and mass spectrometry in the CO pulse (Figure 4a).[13b] CO oxidation by Pd with oxygen from CZ is not exhausted until the end of the CO pulse. The temporal profiles of the Pd/CZ reflections that are shown in Figure 3a,b and the CO_2 evolution (Figure 4c) are very different from those that were observed for Pd/Al_2O_3 and CZ, demonstrating that they are stabilized through contact with CZ. Therefore, an improved resistance towards reduction of the Pd^{2+} species is imparted by the oxygen storage capacity of ceria.

The observation of the metallic Pd phase on the Pd/CZ material by XRD, which was only made at the very end of the CO pulse, is delayed compared to the IR observation, suggesting that the reduced Pd atoms do not form an XRD active phase. On the contrary, adsorption of CO on the metal oxide is already detected by XRD by an increase of approximately 1% in the amount of Ce^{3+} about ten seconds after exposure to CO. The ordered Pd phase grows and persists during the O_2 pulse before vanishing synchronously with Ce re-oxidation. Ce^{3+} acts as a sink for oxygen, and Pd oxidation commences only after Ce^{3+} re-oxidation.

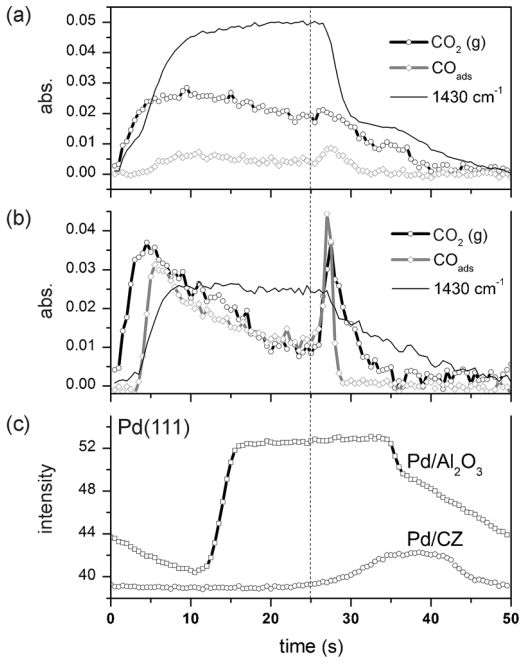

Figure 4. DRIFT data during a full CO/O_2 modulation period for a) Pd/CZ and b) Pd/Al_2O_3 revealing CO_2 evolution (2364 cm^{-1}), the amount of CO_{ads} [measured as the difference between the CO_B signals at 1904 cm^{-1} and 1927 cm^{-1} (1941 cm^{-1} for Pd/Al_2O_3)], and the presence of carbonate species (observed at ca. 1430 cm^{-1}; scaled by a factor of five). c) Temporal response of the Pd(111) reflections of Pd/CZ and Pd/Al_2O_3.

Only the phase-angle dependence of the reflections shown in Figure 3 can disclose detailed information on the kinetics of these processes. Whereas the large phase lag ($\Delta\phi^{PSD} = 190°$) between the PdO (2.37 $Å^{-1}$) and Pd (2.78 $Å^{-1}$) reflections is obvious in Pd/Al_2O_3 and reflects the conversion of one species into the other (Figure 3e), the small phase lag, which is only measurable by PSD, between the reflections of CZ and that of metallic Pd ($\Delta\phi^{PSD} = 20°$) suggests that Pd^0 evolves (and Pd^{2+} is reduced) before a change in the d spacing of CZ becomes detectable (Figure 3c,d). This key observation implies a direct interaction of Pd^{2+} and CZ rather than discrete oxygen transfer between the components. The difference becomes more evident by using PSD at higher harmonics, where faster processes can be more easily captured, unfortunately at the expense of intensity (Figure S6).[17] A phase lag of $\Delta\phi^{PSD} = 50°$ is observed for $k = 5$. This information is not accessible by analyzing the raw time-resolved HXRD data.

The delayed reduction of Pd is supported by a similar quick EXAFS experiment (Figure S7) using the same cell and setup. The levels of Pd^{2+} versus Pd^0 obtained from linear combination analysis (LCA; Figure S8) of the Pd K-edge XANES spectra using bulk PdO and Pd foil as reference samples closely follow the overall temporal behavior of the Pd(111) reflection. The use of bulk PdO as a reference is evidently an approximation in the case of Pd/CZ because a well-defined PdO phase has not been detected. Nevertheless, the XANES/LCA data qualitatively matches the general behavior extracted from HXRD. A crucial result is that reduction of Pd/CZ is relative to the start of the CO pulse, and significant Pd reduction is only observed towards the end of the pulse. Furthermore, the reduced state of Pd/CZ also persists after switching from CO to O_2, as observed in the modulation HXRD data. Therefore, the HXRD and XAS results are in striking agreement with respect to the kinetics of the Pd redox process.

Aside from adsorbed CO, which is readily formed after addition of CO to both catalysts, a variety of adsorbed carbonate species (1700–1200 cm^{-1}) appear, which dominate the IR spectra of Pd/CZ (Figure S5). Their temporal behavior, which is well represented by the evolution of the signal at 1430 cm^{-1} (Figure 4a,b), shows that carbonate species are removed much more slowly from the catalysts than CO. Four seconds after the $CO \rightarrow O_2$ switch, all adsorbed Pd–CO species have disappeared, that is, much earlier than the disappearance of the metallic Pd phase as determined by HXRD. The removal of adsorbed CO species upon the $CO \rightarrow O_2$ switch is fast and matches the second CO_2 production event in both catalysts. At this point in time, when gas-phase oxygen is consumed and CO_2 is formed, the reduction of Pd^{2+} and ceria becomes visible by XRD (and XAS), indicating that oxygen is

not yet able to re-oxidize the two components. Oxygen dissociation on Pd followed by spill-over to Ce^{3+}, which occurs simultaneously to the slower direct dissociation at Ce^{3+} defects, retards the formation of Pd–O bonds (Pd/CZ) or PdO (Pd/Al_2O_3). The presence of carbonate-like species in the O_2 pulse seems to correlate with the reduced state of the catalysts, indicating that their removal is the limiting step for catalyst (specifically for CZ) re-oxidation.

In conclusion, the presented approach provides vastly superior sensitivity and specificity towards extremely subtle and perhaps operationally deterministic structure–reactivity changes that occur in a complex system operating under realistic conditions. The application of phase-sensitive detection (PSD) to synchrotron HXRD can push the detection limits beyond those that are generally accepted. PSD is able to enhance our perception of structural changes that are associated with a subset of the complete material and separates the contributions of two reactively distinct phases (CZ and Pd). The complete kinetic behavior of small noble-metal nanoparticles residing upon extremely heavy support materials is typically not discernible by microscopic (Z contrast) and diffraction methods (length scales, support contributions), but becomes accessible with these experiments. The intrinsic advantage of XRD is that it can deliver a global description of a complex catalyst at work; for example, it simultaneously elucidates the structures of the Pd nanoparticles and the metal oxide support. Such enhanced insights should be achievable in all systems that involve functional materials where reversible cycling (the modulation) of one or more of the intrinsic process variables may be achieved.

Received: March 7, 2014
Published online: June 5, 2014

Keywords: ceria · modulation · palladium · time-resolved studies · X-ray diffraction

[1] J. Hanson, P. Norby in *In situ characterization of heterogeneous catalysts* (Eds.: J. A. Rodriguez, J. C. Hanson, P. J. Chupas), Wiley, Hoboken, **2013**, p. 121.
[2] S. Bordiga, E. Groppo, G. Agostini, J. A. van Bokhoven, C. Lamberti, *Chem. Rev.* **2013**, *113*, 1736.
[3] J. C. Yang, M. W. Small, R. V. Grieshaber, R. G. Nuzzo, *Chem. Soc. Rev.* **2012**, *41*, 8179.
[4] a) D. Baurecht, U. P. Fringeli, *Rev. Sci. Instrum.* **2001**, *72*, 3782; b) T. Bürgi, A. Baiker, *J. Phys. Chem. B* **2002**, *106*, 10649; c) N. Maeda, K. Hungerbühler, A. Baiker, *J. Am. Chem. Soc.* **2011**, *133*, 19567.
[5] T. Bürgi, *J. Catal.* **2005**, *229*, 55.
[6] a) D. Ferri, S. K. Matam, R. Wirz, A. Eyssler, O. Korsak, P. Hug, A. Weidenkaff, M. A. Newton, *Phys. Chem. Chem. Phys.* **2010**, *12*, 5634; b) D. Ferri, M. A. Newton, M. Nachtegaal, *Top. Catal.* **2011**, *54*, 1070; c) C. F. J. König, J. A. van Bokhoven, T. J. Schildhauer, M. Nachtegaal, *J. Phys. Chem. C* **2012**, *116*, 19857; d) C. F. J. König, T. J. Schildhauer, M. Nachtegaal, *J. Catal.* **2013**, *305*, 92.
[7] a) D. Chernyshov, W. van Beek, H. Emerich, M. Milanesio, A. Urakawa, D. Viterbo, L. Palin, R. Caliandro, *Acta Crystallogr. Sect. A* **2011**, *67*, 327; b) W. van Beek, H. Emerich, A. Urakawa, L. Palin, M. Milanesio, R. Caliandro, D. Viterbo, D. Chernyshov, *J. Appl. Crystallogr.* **2012**, *45*, 738; c) R. Caliandro, D. Chernyshov, H. Emerich, M. Milanesio, L. Palin, A. Urakawa, W. van Beek, D. Viterbo, *J. Appl. Crystallogr.* **2012**, *45*, 458; d) D. Ferri, M. A. Newton, M. Di Michiel, S. Yoon, G. L. Chiarello, V. Marchionni, S. K. Matam, A. Weideklaff, F. Wen, J. Gieshoff, *Phys. Chem. Chem. Phys.* **2013**, *15*, 8629.
[8] M. A. Newton, M. Di Michiel, A. Kubacka, M. Fernandez-Garcia, *J. Am. Chem. Soc.* **2010**, *132*, 4540.
[9] G. Fagherazzi, P. Canton, P. Riello, N. Pernicone, F. Pinna, M. Battagliarin, *Langmuir* **2000**, *16*, 4539.
[10] a) Z. Kaszkur, *J. Appl. Crystallogr.* **2000**, *33*, 1262; b) J. D. Grunwaldt, N. van Vegten, A. Baiker, *Chem. Commun.* **2007**, 4635; c) F. Hasché, M. Oezaslan, P. Strasser, *ChemPhysChem* **2012**, *13*, 828.
[11] Phase-sensitive detection (PSD):
$I_k^{\phi^{PSD}}(e) = \frac{2}{T}\int_0^T I(e,t)\sin(k\pi t + \phi_k^{PSD})\mathrm{d}t$
where T is the length of one period, $\bar{\omega}$ is the modulation frequency, k is the demodulation index ($k=1$), ϕ_k^{PSD} is the demodulation phase angle for a $k\bar{\omega}$ demodulation, and $I(t)$ and I_k are the responses in the time and phase domains, respectively. A more specific equation for modulated-excitation X-ray diffraction is given in Ref. [7c].
[12] a) A. Trovarelli, *Catalysis by ceria and related materials*, Imperial College Press, London, **2002**; b) A. Trovarelli, C. de Leitenburg, M. Boaro, G. Dolcetti, *Catal. Today* **1999**, *50*, 353; c) W. C. Chueh, C. Falter, M. Abbott, D. Scipio, P. Furler, S. M. Haile, A. Steinfeld, *Science* **2010**, *330*, 1797; d) G. Vilé, B. Bridier, J. Wichert, J. Perez-Ramirez, *Angew. Chem.* **2012**, *124*, 8748; *Angew. Chem. Int. Ed.* **2012**, *51*, 8620.
[13] a) Y. Nagai, K. Dohmae, Y. Ikeda, N. Takagi, T. Tanabe, N. Hara, G. Gilera, S. Pascarelli, M. A. Newton, O. Kuno, H. Jiang, H. Shinjoh, S. Matsumoto, *Angew. Chem.* **2008**, *120*, 9443; *Angew. Chem. Int. Ed.* **2008**, *47*, 9303; b) M. A. Newton, M. Di Michiel, A. Kubacka, A. Iglesias-Juez, M. Fernandez-Garcia, *Angew. Chem.* **2012**, *124*, 2413; *Angew. Chem. Int. Ed.* **2012**, *51*, 2363; c) M. Hatanaka, N. Takahashi, N. Takahashi, T. Tanabe, Y. Nagai, A. Suda, H. Shinjoh, *J. Catal.* **2009**, *266*, 182.
[14] S. K. Matam, A. Eyssler, P. Hug, N. van Vegten, A. Baiker, A. Weidenkaff, D. Ferri, *Appl. Catal. B* **2010**, *94*, 77.
[15] H. P. Klug, L. E. Alexander, *X-ray diffraction procedure for policrystalline and amorphous materials*, Wiley, New York, **1954**.
[16] A. Martorana, G. Deganello, A. Longo, F. Deganello, L. Liotta, A. Macaluso, G. Pantaleo, A. Balerna, C. Meneghini, S. Mobilio, *J. Synchrotron Radiat.* **2003**, *10*, 177.
[17] V. Marchionni, M. A. Newton, A. Kambolis, S. K. Matam, A. Weidenkaff, D. Ferri, *Catal. Today* **2014**, *229*, 80.

